

# THERMODYNAMIC PERFORMANCE OF A THERMAL VAPOR COMPRESSION REFRIGERATION UNIT

Giuma Fellah, Abdurrauf Nass and Abdussalam Awid

Department of Mechanical and Industrial Engineering,  
Faculty of Engineering, University of Tripoli  
E-mail: gfellah2008@yahoo.com

## الملخص

تهدف هذه الورقة إلى تقييم الأداء الديناميكي الحراري لوحدة تبريد بالضغط الحراري للبخار. يتم في هذا النوع من الدوائر الاستغناء عن الضاغط الميكانيكي، ويستخدم قاذف (Ejector) عوضاً عنه، حيث يقوم القاذف بضغط البخار حرارياً إلى الضغط المطلوب للمكثف. لتقييم الأداء الديناميكي الحراري، تمت محاكاة وحدة التبريد باستخدام موائع تبريد مختلفة عند درجات حرارة مختلفة للمصدر والمبخر.

يمكن استخدام الطاقة المنخفضة الجودة في تشغيل وحدات التبريد من هذا النوع، حيث توجد كميات كبيرة من الطاقة الحرارية يتم طردها عادة للمحيط الجوي، والتي تزيد من مشكلة التلوث الحراري للبيئة، مثال على ذلك غازات العادم في محطات التربينات الغازية والوحدات الصناعية. كما تتوفر كميات كبيرة من الطاقة الشمسية والجوفية التي يمكن استغلالها لتشغيل هذا النوع من منظومات التبريد.

جذبت منظومات التبريد بالقاذف الكثير من البحوث، وتستخدم هذه المنظومات عادة الماء كمائع تشغيل بمعامل أداء منخفض، مع إمكانية استخدام موائع تبريد أخرى لتحسين الأداء، حيث تم اختبار موائع تبريد مثل R114 و R141b, R152a, R123 لتشغيل دوائر التبريد، وفيها أُدرت نسبة الجر ونسبة المساحة ومعامل الأداء تحت ظروف تشغيلية مختلفة.

## ABSTRACT

The objective of this paper is to evaluate the thermodynamic performance of a refrigeration unit in which the simple vapor compression refrigeration cycle is replaced by an ejector where the refrigerant is compressed thermally to the desired condenser pressure.

Different refrigerants operating under different source and evaporator temperatures are simulated to predict the unit performance. Low quality waste heat is used to power the refrigeration unit. There is a great deal of waste heats being released into environment, such as exhaust gas from turbines and engines, and waste heat from industrial plants, which cause thermal environmental pollution. In addition, there are also abundant geothermal resources and solar energy available in the world.

Ejector refrigeration systems have attracted many research activities in recent years. These systems traditionally operate with water as the refrigerant with low COP values. Other refrigerants commonly used in mechanical vapor compression cycles may provide better performance for ejector refrigeration cycles.

Refrigerants such as R141b, R152a, R123 and R114 are chosen as working fluids in an ejector refrigeration system. The entrainment ratio, area ratio and the coefficient of performance are estimated and compared for different refrigerants and operating conditions.

**KEYWORDS:** Refrigeration; Thermal Vapor Compression; Entrainment Ratio; Coefficient of Performance; Exergy.

## INTRODUCTION

In recent years, there is a vast amount of waste heat being released into atmosphere, such as exhaust gas from turbines and engines, and waste heat from industrial plants, which lead to severe environmental pollution. In addition, there are also abundant geothermal resources and solar energy existing in the world.

In order to exploit these waste heat and renewable energy for their potential in reducing fossil fuel consumption and alleviating environmental problems, ejector refrigeration systems have attracted many research activities [1]. These systems have numerous advantages over the traditional vapor compression system. One important advantage is the fact that such systems require no moving part other than the pump and hence no lubrication required [2].

Most of conventional refrigeration systems based on vapor compression cycle are driven by high-grade mechanical energy and electrical energy. The most attractive attribute of ejector refrigeration system over the conventional refrigeration system that it can be driven by low-grade thermal energy such as solar energy, waste industrial heat and geothermal energy. Compared to other renewable energy operated refrigeration system, ejector refrigeration system has simplicity, is simpler more reliable, has longer life, lower initial and running cost.

The main disadvantage of ejector refrigeration system is the low coefficient of performance (COP) when compared to others refrigeration cycle such as absorption refrigeration cycle. The performance of ejector refrigeration system mainly depends on the thermodynamic property of working fluid [3]. In addition, these systems are heat powered, therefore, waste heat, solar heat, biomass or geothermal energy can be utilized via these systems. Inexpensive thermal energy sources can make an ejector refrigeration system a viable and economic proposition [2].

Many research works have been carried out to study the performance of ejector refrigeration cycle with different refrigerants [3]. Traditionally, ejector refrigeration systems operate with water as refrigerant. However, halocarbon compound refrigerants have been widely used in ejector refrigeration systems for higher COP values.

Huang and Chang (1999) [4] derived two empirical correlations from the test results of 15 ejectors for the performance prediction of ejectors using R141b as the working fluid. The prediction of the entrainment ratio  $\omega$  using the correlations is within  $\pm 10\%$  error.

Huang et al (1998) [5] develop high-performance solar ejector cooling system using R141b as the working fluid. They obtained experimentally a COP of 0.5 for a single-stage ejector cooling system at a generating temperature of 90°C, condensing temperature of 28°C, and an evaporating temperature 8°C.

Kumar and Jain (2013) [6] developed mathematical a model in Engineering Equation Solver (EES) software for single phase Ejector Refrigeration System. The model is then used to determine the performance of natural refrigerants R717 and Propane.

Reddick, et al (2012) [7] studied experimentally the possibility of improving the energy efficiency of a vapor compression refrigeration system where a two-phase ejector replaces the expansion valve. A test bench using refrigerant R134a was designed and built which functions in both the conventional mode and in ejector mode. Experimental results showed an improvement of 11% in the coefficient of performance (COP) in ejector mode as compared with the conventional mode.

Kshirsagar and Deshmukh (2013) [8] presented the latest developments of the ejector refrigeration and combined vapor compression-ejector refrigeration systems.

Zhenga, et al (2012) [9] established a simulation program about the solar ejector system performance. The characteristic of entrainment ratio has been analyzed when the R134a, R290 and R718 are adopted as working fluid respectively. It is found that the entrainment ratio of R290 is the biggest over the range of operating conditions, and the entrainment ratio of R134a is the middle, and the R718's is the least.

Zhengshu Dai, et al (2012) [10] studied a pump-less ejector refrigeration system driven by solar thermal energy, and R134a is proposed as refrigerant. The prototype is constructed and the performance of the ejector, which is used in a pump-less system, is investigated experimentally. The design condition of the pump-less ejector refrigeration system is: evaporation temperature of 15°C, condensation temperature of 45°C, generation temperature of 80°C, and refrigeration capacity of 1.5 kW. The influence of the evaporation temperature, condensation temperature and generation temperature on the performance of the ejector is studied. Results show that the performance of the tested ejector is not good, and suggestions for improving the performance of the ejector are made. Thermal compression refrigeration cycle could be employed for vehicle air conditioning by utilizing the exhaust gases to power the cycle.

This paper aims to find the most suitable refrigerant for the best thermodynamic performance of an ejector refrigeration, where several refrigerants are theoretically tested to evaluate the thermodynamic performance of thermal compression refrigeration cycle.

## **MODELING OF THERMAL VAPOR COMPRESSION REFRIGERATION UNIT**

### **Operational mode of the ejector [11]**

The ideal gas behavior is assumed for the refrigerant vapor flowing inside the ejector. The ejector performance can be divided into three operational modes, according to the backpressure  $P_c$  [11], see Figure (1):

- double-choking or critical mode as  $P_c \leq P_c^*$ , while the primary and the entrained flows are both choking and the entrainment ratio is constant, i.e.  $\omega$  constant;
- single-choking or subcritical mode as  $P_c^* < P_c < P_{co}$ , while only the primary flow is choked and  $\omega$  changes with the back pressure  $P_c$ ; and
- back-flow or malfunction mode as  $P > P_{co}$ , while both the primary and the secondary flow are not choked and the entrained flow is reversed (malfunction), i.e.  $\omega \leq 0$ . Figure (2) shows the schematic diagram of the thermal vapor compression cycle. It consists of evaporator, ejector, condenser, pump, expansion valve and heat exchanger for heat recovery. The cycle is powered by supplying heat to the refrigerant through the heat

recovery vapor generator. The heat exchanger receives heat from an external source such as solar collector or the exhaust gases of an industrial plant. The primary vapor from the heat exchanger at (g) is accelerated through the nozzle of the ejector and creates low pressure at the nozzle exit state (1), see Figure (3).

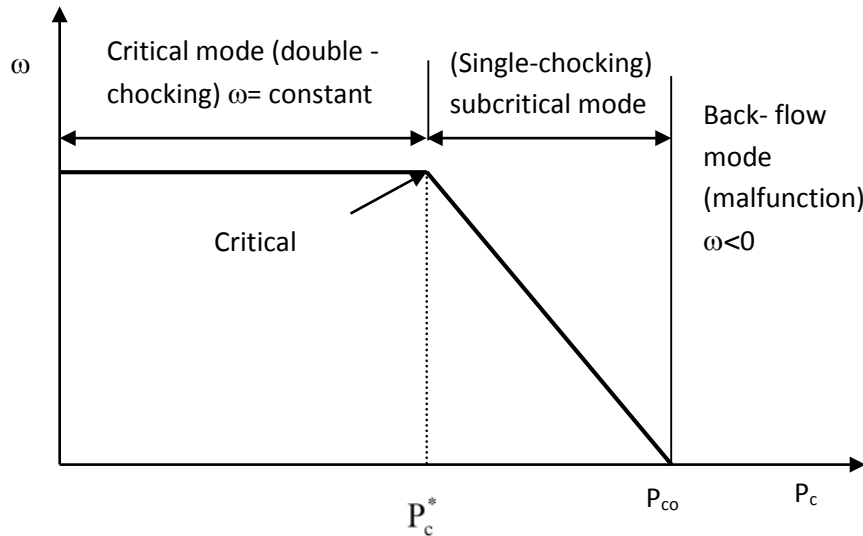


**Figure 1: Operational mode of ejector [11]**

Due to pressure differences between states (1) and e, the refrigerant flows from the evaporator into the ejector. The two streams are mixed in the mixing zone between the nozzle exit at (section y-y) and section (m-m). The mixed stream becomes supersonic in the mixing zone. To avoid shock at the diffuser exit (condenser inlet) a transverse shock occurs along the constant cross sectional area duct (at section (s-s) for example). After shock, the velocity of the mixed stream becomes subsonic and is further reduced in the diffuser.

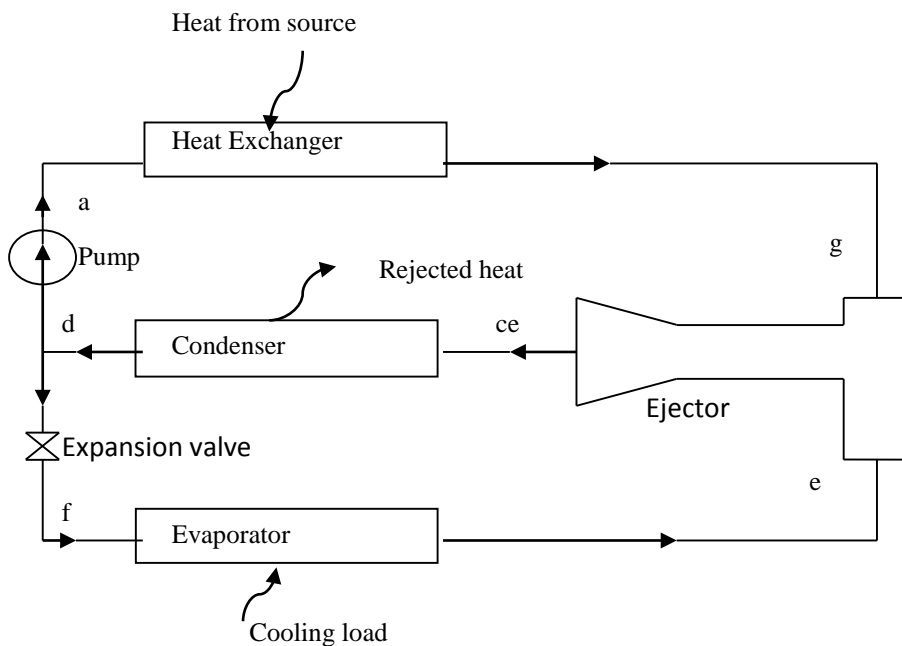


**Figure 2: Ejector-Refrigeration System.**

### The mathematical model [11]

Assume one dimensional flow of gas within the ejector.

#### The primary flow:

The mass flow rate of the primary motive flow may be found as:

$$m_g = P_g \times A_t \sqrt{\frac{\eta_p \gamma}{T_g R} \left( \frac{2}{\gamma + 1} \right)^{\frac{\gamma+1}{\gamma-1}}} \quad (1)$$

Where  $p_g$  = pressure for the primary motive flow,  $A_t$  = throat area,  $T_g$  = generator temperature,  $R$  = gas constant,  $\gamma$  = specific heat ratio and  $\eta_p$  is a coefficient relating to the isentropic efficiency of the compressible flow in the nozzle. The Mach number of the primary  $M_{p1}$  at the nozzle exit can be found by the trial and error from the following equation:

$$\left( \frac{A_{pl}}{A_t} \right)^2 = \frac{1}{M_{pl}^2} \left[ \frac{2}{\gamma+1} \left( 1 + \frac{\gamma-1}{2} M_{pl}^2 \right) \right]^{\frac{\gamma+1}{\gamma-1}} \quad (2)$$

Where  $A_{p1}$  is the nozzle exit area. The pressure at the nozzle exit can be found as:

$$P_{p1} = \frac{P_g}{\left( 1 + \frac{\gamma-1}{2} M_{pl}^2 \right)^{\frac{\gamma}{\gamma-1}}} \quad (3)$$

Where  $P_{p1}$  = pressure at the nozzle exit.

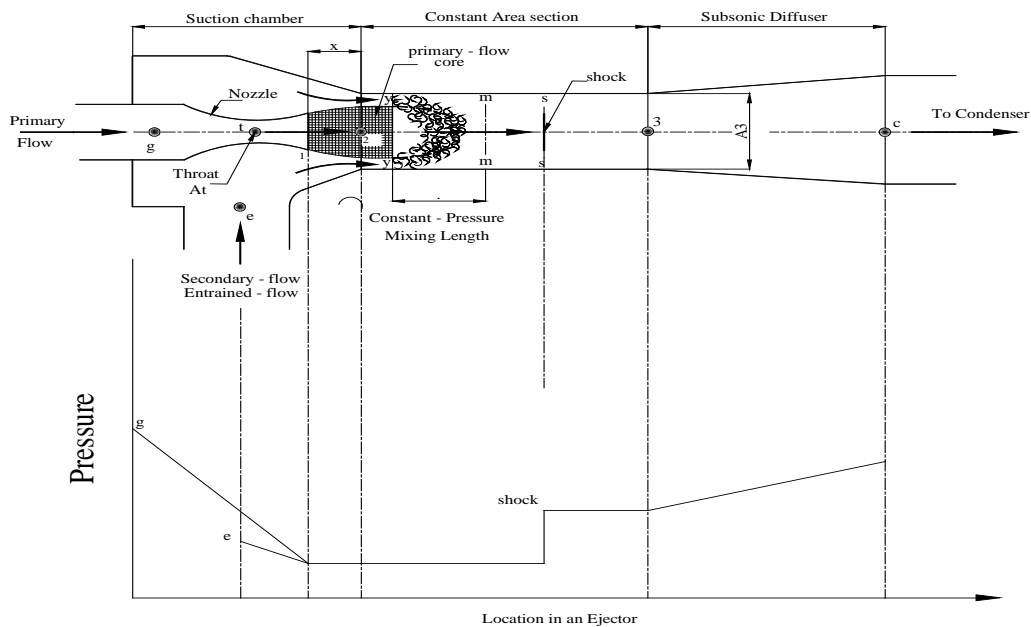


Figure 3: Ejector and pressure profile.

The Mach number  $M_{py}$  of the primary flow at the y-y section is:

$$M_{py} = \left[ \frac{1 + \frac{(\gamma-1)}{2} M_{p1}^2}{\left( \frac{P_{py}}{P_{p1}} \right)^{\frac{\gamma-1}{\gamma}} - 1} \left( \frac{2}{\gamma-1} \right) \right]^{0.5} \quad (4)$$

Where  $p_{py}$ = pressure of the primary flow at y-y section. The cross sectional area of the primary flow ( $A_{py}$ ) at y-y section is:

$$A_{py} = A_{p1} \frac{\left( \frac{\phi_p}{M_{py}} \right) \left[ \left( \frac{2}{\gamma+1} \right) \left[ 1 + \frac{\gamma-1}{2} (M_{py})^2 \right]^{\frac{\gamma+1}{2(\gamma-1)}} \right]}{\frac{1}{M_{p1}} \left[ \left( \frac{2}{\gamma+1} \right) \left[ 1 + \frac{\gamma-1}{2} (M_{p1})^2 \right]^{\frac{\gamma+1}{2(\gamma-1)}} \right]} \quad (5)$$

$\phi_p$ = coefficient accounting for the frictional loss.

### The entrained flow:

The mass flow rate of the secondary entrained flow may be found:

$$m_{sy} = P_e A_{sy} \sqrt{\frac{\eta_s \gamma}{T_e R} \left( \frac{2}{\lambda+1} \right)^{\frac{\gamma+1}{\gamma-1}}} \quad (6)$$

Where:  $P_e$ = evaporator pressure  $T_e$ = evaporator Temperature and  $\eta_s$  is a coefficient relating to the isentropic efficiency of the compressible flow in the nozzle. The pressure in the entrained flow can be found from:

$$P_{sy} = \frac{P_e}{\left( 1 + \frac{[\gamma-1]}{2} M_{sy}^2 \right)^{\frac{\gamma}{\gamma-1}}} \quad (7)$$

Where:  $M_{sy}$ = Mach number of entrained flow at section y-y.  $A_3$  is the total cross sectional area at section y-y, and equal to:

$$A_3 = A_{py} + A_{sy} \quad (8)$$

The temperature of the primary flow ( $T_{py}$ ) at section y-y is:

$$T_{py} = \frac{T_g}{\left( 1 + \frac{\gamma-1}{2} M_{py}^2 \right)} \quad (9)$$

The temperature of the secondary flow ( $T_{sy}$ ) at section y-y is:

$$T_{sy} = \frac{T_e}{\left( 1 + \frac{\gamma-1}{2} M_{sy}^2 \right)} \quad (10)$$

**Mixing section:**

The two streams start to mix at section y–y. A shock occurs with a sharp pressure rise at section s–s. By applying the momentum equation it is found:

$$\phi_m (m_g V_{py} + m_s V_{sy}) = (m_g + m_s) V_m \tag{11}$$

Or

$$V_m = \phi_m \frac{(m_g V_{py} + m_s V_{sy})}{(m_g + m_s)} \tag{12}$$

Where:  $V_{sy}$  = velocity of entrained flow at section y-y,  $V_{py}$ = velocity of primary flow at section y-y and  $V_m$ = velocity of the mixed flow. From the energy balance we may have:

$$T_m = \left( \frac{m_g \left( C_p \cdot T_{py} + \frac{V_{py}^2}{2} \right) + m_e \left( C_p \cdot T_{sy} + \frac{V_{sy}^2}{2} \right)}{(m_g + m_e)} - \frac{V_m^2}{2} \right) / C_p \tag{13}$$

The gas velocities at the y-y section and s-s section are:

$$V_{py} = M_{py} a_{py} \tag{14-a}$$

$$a_{py} = \sqrt{\gamma R T_{py}} \tag{14-b}$$

$$V_{sy} = M_{sy} a_{sy} \tag{15-a}$$

$$a_{sy} = \sqrt{\gamma R T_{sy}} \tag{15-b}$$

The Mach number of the mixed flow can be found using the following relation:

$$M_m = \frac{V_m}{a_m} \tag{16-a}$$

$$a_m = \sqrt{\gamma R T_m} \tag{16-b}$$

Where:  $a_{py}$ = sonic velocity of primary flow,  $a_{sy}$ = sonic velocity of entrained flow and  $M_m$ = Mach number of mixed flow. The mixed flow a cross section m–m to section 3–3. A normal shock will take place at section s–s with a sharp pressure rise. The pressure at section 3-3 is:

$$P_3 = P_m \left[ 1 + \frac{2\gamma}{\gamma+1} \left[ (M_m)^2 - 1 \right] \right] \tag{17}$$

Where  $P_m$ = pressure at mixing section and  $P_3$ = pressure at section 3-3. The Mach number at section 3-3 is:

$$M_3 = \left[ \frac{1 + \left( \frac{\gamma-1}{2} \right) M_m^2}{\left( \gamma M_m^2 - \frac{\gamma-1}{2} \right)} \right]^{0.5} \tag{18}$$

Where:  $M_m$  is the Mach number of the mixed flow through diffuser. The pressure at the exit of the diffuser is:

$$P_c = P_3 \left( 1 + \frac{\gamma - 1}{2} M_3^2 \right)^{\frac{\gamma}{\gamma - 1}} \quad (19)$$

The performance of an ejector is generally defined in terms of the mass flow ratio between the streams (from the evaporator) and the generator; this ratio is called the entrainment ratio  $\omega$  and written as:

$$\omega = \frac{m_s}{m_g} \quad (20)$$

The P-h diagram for the selected system is shown in Figure (4).

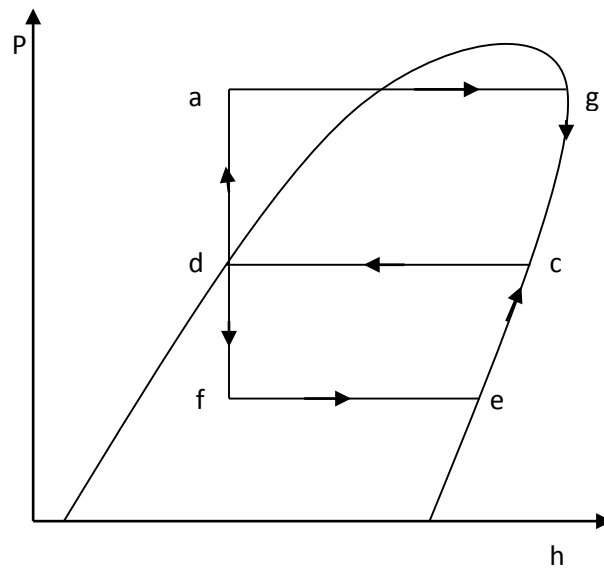


**Figure 4: Pressure –Specific enthalpy diagram**

The coefficient of performance can be written as:

$$\text{COP}^{\text{1st}} = \omega \left( \frac{h_e - h_f}{h_g - h_a} \right) \quad (21)$$

The coefficient of the cycle performance exergy is:

$$\text{COP}^{\text{exergy}} = \left| Q_L \left( 1 - \frac{T_0}{T_L} \right) \right| / \left| Q_H \left( 1 - \frac{T_0}{T_H} \right) \right| \quad (22)$$

Here  $T_H$  represents the source temperature and  $T_L$  is the cooling space temperature. For reversible heat transfer,  $T_H$  almost equal to  $T_g$  and  $T_L$  almost equal to  $T_e$ .

To demonstrate the advantage of using thermal vapour compression refrigeration cycle over simple mechanical compression refrigeration cycle from energy saving point of view, let the two cycles have the same cooling load and first law coefficient of performance, then:

$$\left(\frac{Q_L}{Q_H}\right)_{TVC} = \left(\frac{Q_L}{W}\right)_{MC} \quad (23)$$

If  $\varepsilon$  is the conversion efficiency of the heat engine which produces the mechanical power to operate the mechanical compression refrigeration cycle, then:

$$\left(\frac{Q_L}{Q_H}\right)_{TVC} = \left(\frac{Q_L}{\varepsilon Q_H}\right)_{MC} \quad (24)$$

And hence:

$$\frac{Q_{H,MC}}{Q_{H,TVC}} = \frac{1}{\varepsilon} \quad (25)$$

## RESULTS AND DISCUSSIONS

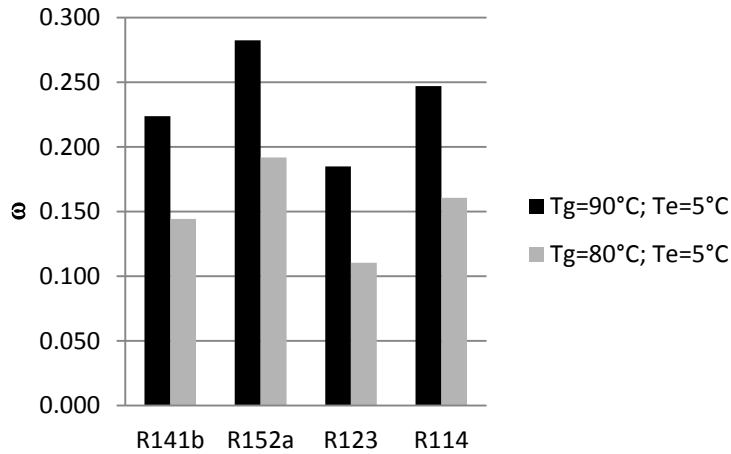
The thermodynamic performance of a thermal vapor compression refrigeration unit is presented. Different kinds of refrigerant are tested under different operating conditions. Entrainment ratio, ejector area ratio and coefficient of performance based on first law and exergy are obtained.

Two source temperatures that are suitable for waste heat or solar energy applications of 90°C and 80°C are adopted for the analysis. Also for the evaporator, two temperatures of 5°C and 0.0°C which are proper for chilling applications are selected for the analysis. The condenser inlet temperature (that is the outlet ejector temperature) is found by calculating the ejector outlet pressure (condenser pressure) and by calculating the enthalpy at the ejector outlet (condenser inlet). Area ratios are altered during calculation until suitable pinch point between the condenser temperature and environmental temperature is obtained.

### Results based on source temperature of 90°C; 80°C and evaporator temperature of 5°C.

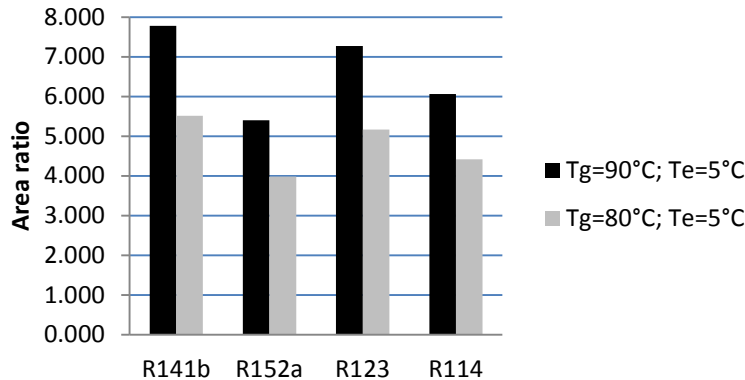
Figure (5) shows the ejector entrainment ratio for various refrigerants. As it can be seen, the entrainment ratio depends on source temperature and on refrigerant kind. Typical values between 0.192 and 0.283 are obtained. Differences are mainly due to properties differences. Low entrainment ratio implies relatively large driving flow for the ejector.

To focus on the influence of source temperature on the entrainment ratio, the source temperature is lowered to 80°C and the evaporator temperature is kept at 5°C. Both temperature and saturation pressure affect the entrainment ratio. Lowering the source temperature would lower the saturation pressure. Based on equations (1), (6) and (20), slight decrease in the entrainment ratio is predicted.



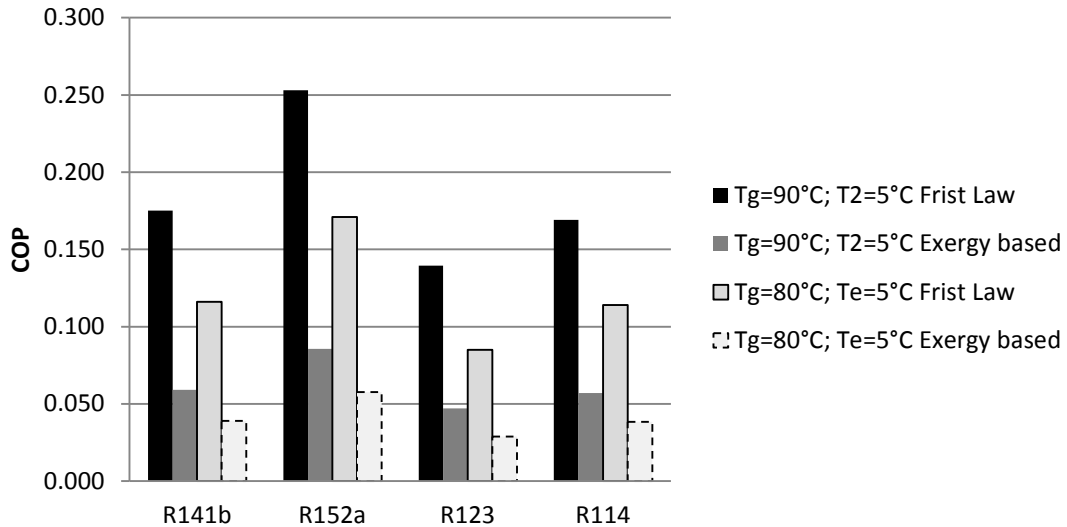
**Figure 5: Entrainment ratios for source temperature of 90°C and evaporator temperature of 5°C**

Figure (6) shows ejector area ratios for various refrigerants. For 90°C source temperature, values between 5.40 and 7.78 are obtained. These values are close to those reported in the literature. Ejector area ratio is influenced by the entrainment ratio. Smaller area ratio is expected as we lower the source temperature to 80°C.



**Figure 6: Ejector area ratios for various refrigerants for source temperature of 90°C and evaporator temperature of 5°C**

The coefficients of performance based on the first law and exergy are shown in Figure (7). COP values for the given operating conditions are mainly influenced by the ejector entrainment ratio [2]. Low COPs are obtained, and hence poor thermodynamic performance characterizes thermal vapor compression refrigeration units. Reducing the source temperature to 80°C alter both the entrainment ratio and the enthalpy change of the refrigerant crosses the heat exchanger, and hence affects the coefficient of performance, see equation (2). Lower COPs are obtained by reducing the source temperature to 80°C.



**Figure 7: Coefficients of performance based on the first law and exergy for source temperature of 90°C and evaporator temperature of 5°C**

**Results based on evaporator temperature of 0°C and source temperature of 90°C and 80°C**

To analyze the effect of the evaporator temperature, it is lowered to 0°C. Lowering the evaporator temperature would reduce the saturation pressure and the secondary flow as predicted by equation (6), and hence a decrease in the entrainment ratio is noticed, as shown in Figure (8). The negative entrainment ratios for R141b and R123 indicate a back flow or malfunction, where the condenser pressure ( $P_c$ ) exceeds the limiting pressure ( $P_{co}$ ) of ejector operational mode (case 3, Figure (1)). Hence the corresponding results are omitted for R141b and R123 under this working condition.

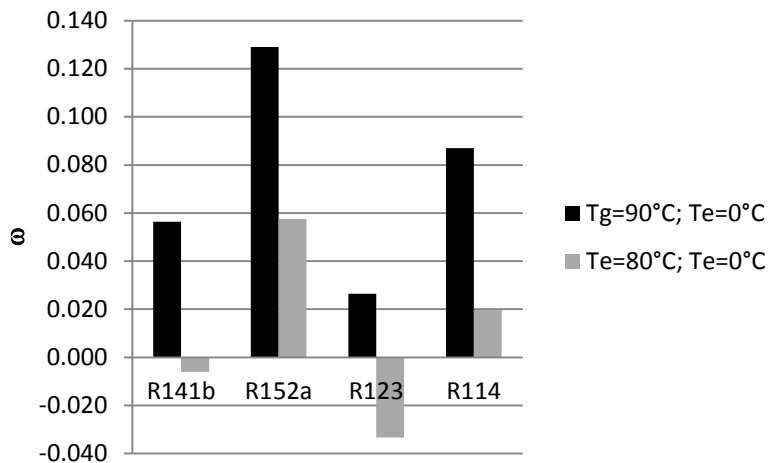


**Figure 8: Ejector entrainment ratios for source temperature of 90°C and evaporator temperature of 0°C**

Figure (9) shows area ratio for different refrigerants. Lower values are obtained by reducing the evaporator temperature; however the trend is identical to 5°C evaporator temperature.

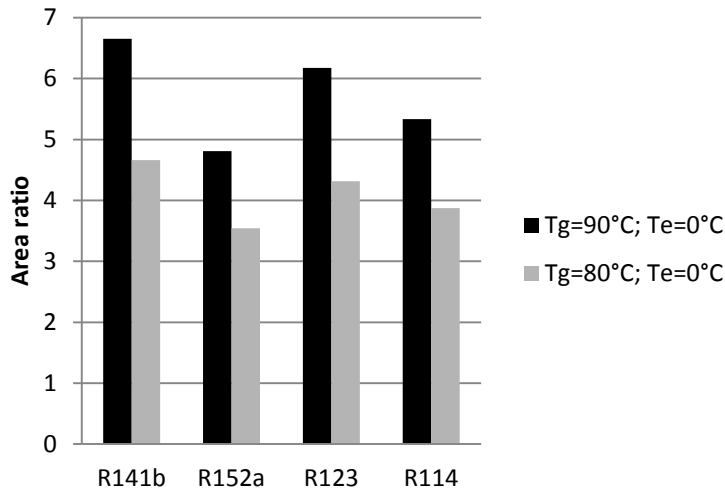


**Figure 9: Ejector area ratios for source temperature of 90°C and evaporator temperature of 0°C**

Differences are related mainly to the properties differences of the refrigerants. For 80°C source temperature, the results for 0.0°C evaporator temperature are quite different from that obtained for 5°C evaporator temperature.

Figure (10) shows the coefficients of performance which are based on the first law and exergy. Lowering the evaporator temperature decreases both the enthalpy change in the evaporator and the entrainment ratio. A substantial decrease in COP is predicted by equation (20).

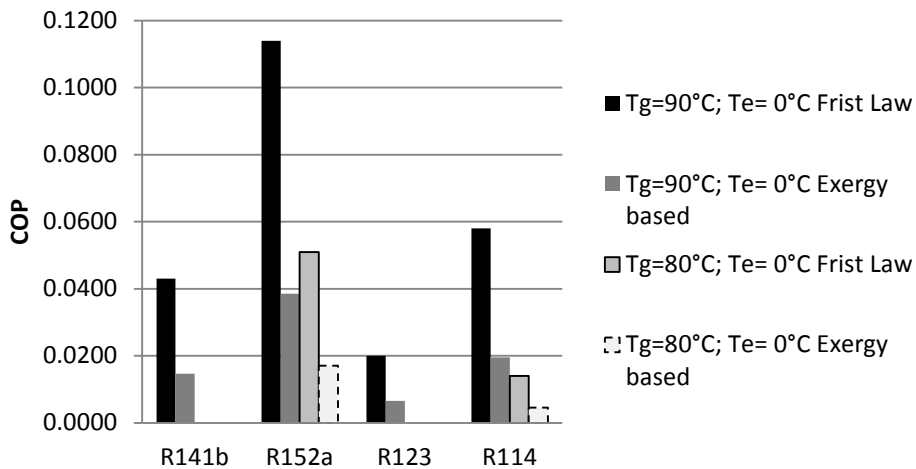


**Figure 10: Coefficients of performance for 90°C source temperature and 0°C evaporator temperature**

The results indicate, vapour compression refrigeration cycles have low COP, and the performance deteriorates by lowering evaporator temperature. The coefficients of

performance based on exergy are lower than the first law based coefficients of performance. The exergy based coefficients of performance, can be interpreted as the potential of doing useful work which gained by the refrigerants, to maximum reversible work that can be done by the heat source. Generally the coefficient of performance of thermal compression refrigeration cycles is relatively low in comparison with simple vapour compression refrigeration cycles.

Figure (11) shows the advantage of using thermal vapour compression refrigeration cycle over simple mechanical compression refrigeration cycle from energy saving point of view. As it can be seen, the driving heat required for unit operation, is greater for mechanical vapour compression units, and ratios decrease with the increase in heat engine conversion efficiency. The ratio will equal to one, when the conversion efficiency of the heat engine becomes 100%, which violate the second law of thermodynamics.

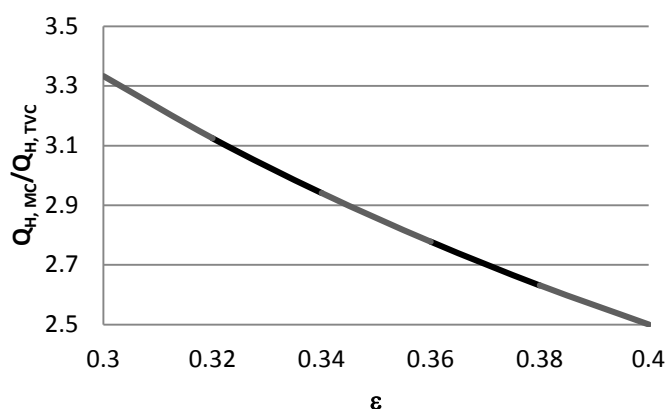


**Figure 11: Heat ratios versus heat engine efficiency**

## CONCLUSIONS

In this paper a refrigeration cycle employing thermal vapor compression ejector is evaluated from the thermodynamics point of view. The following conclusions are drawn:

- The thermal vapor compression refrigeration cycles are characterized by low coefficient of performance when compared to the ordinary vapor compression cycle. However, the operating cost is so low since the driving power of this kind of cycles could be drawn for instance from the exhaust gases of gas turbine cycles, or from solar energy.
- Thermal pollution could be significantly decreased by adopting thermal vapor compression refrigeration cycles.
- Different kinds of refrigerants would produce different thermodynamic performances.
- The source and evaporator temperatures affect the thermodynamic performance of the thermal vapor compression refrigeration cycles.

- To insure better thermodynamic performance, the selection of the refrigerant must be coupled with the operating source and evaporator temperatures.

## REFERENCES

- [1] Dai Y., Wang J. and Gao L. Exergy Analysis, Parametric Analysis and Optimization for a Novel Combined Power and Ejector Refrigeration Cycle. *Applied Thermal Engineering*, 29, 2009, 1983-1990.
- [2] Sun D. Comparative study of the performance of an ejector refrigeration cycle operating with various refrigerants. *Energy Conversion & Management*, 40, 1999, 873-884.
- [3] Gupta R.C. and Kashyap S. Theoretical Study of Ejector Refrigeration System with Working Fluid R410a. *International Journal of Engineering Science and Technology (IJEST)*, 3, 2011, 6508-6512.
- [4] Huang B.J. Chang J.M. Chang. Empirical correlation for ejector design. *International Journal of Refrigeration*, 22, 1999, 379–388
- [5] Huang B. J., Chang J. M., Petrenko V. A. and Zhuk K. B. A Solar Ejector Cooling System Using Refrigerant R141b. *Solar Energy*, 64, 1998, 223–226.
- [6] Kumar J. and Jain N. Performance Analysis of Heat Operated Ejector Refrigeration System with Natural Refrigerants R-717 and Propane. *International Journal of Science and Research* 2, 2013, 139-141.
- [7] Christopher Reddick, Yves Mercadier and Mohamed Ouzzane. Experimental Study of an Ejector Refrigeration System. *International Refrigeration and Air Conditioning Conference at Purdue*, July 16-19, 2012, 2136, 1-10.
- [8] Suhas D. Kshirsagar and M M. Deshmukh. Combined Vapour Compression-Ejector Refrigeration System: A Review. *International Journal of Engineering Research and Development*, 6, 2013, 41-52.
- [9] Huifan Zhenga, Yaohua Lianga and Lanyu Huang. Analysis of Entrainment Ratio about Solar Ejector Refrigerant System. *International Conference on Future Energy, Environment, and Materials. Energy Procedia* 16, 2012, 516 – 521.
- [10] Zhengshu Dai, Yijian He, Yunzhou Huang, Liming Tang and Guangming Chen. Ejector Performance of a Pump-less Ejector Refrigeration System Driven by Solar Thermal Energy. *International Refrigeration and Air Conditioning Conference*, July 16-19, 2012, 2412, 1-9.
- [11] B.J. Huang, J.M. Chang, C.P. Wang and V.A. Petrenko. A 1-D Analysis of Ejector Performance. *International Journal of Refrigeration*, 22, 1999, 354–364.

## NOMENCLATURE

a	Sonic velocity, (m/s).
A	Area, (m <sup>2</sup> ).
C <sub>p</sub>	Specific heat of a gas at constant pressure, (kJ/kg.K).
COP	Coefficient of performance.
h	Enthalpy, (kJ/kg).
$\dot{m}$	Mass flow rate, (kg/s).
M	Mach number.
P	Pressure, (kPa).
P <sub>c</sub> *	Critical back pressure of the ejector, (kPa)
Q	Rate of heat transfer, (kW).
R	Gas constant, (kJ/kg.K)
T	Temperature, (K).
V	Gas velocity, (m/s).

## Greek letters:

$\gamma$	Specific heat ratio.
$\eta$	coefficient relating to the isentropic efficiency of the compressible flow in the nozzle
$\varepsilon$	efficiency
$\emptyset$	Coefficient accounting for the frictional loss.
$\omega$	Entrainment ratio.

## Subscripts

3	Exit of the constant-area section.
c	Exit of ejector; condenser.
co	limiting condition of ejector operational mode
e	Inlet port of the entrained flow; hypothetical throat.
g	Nozzle inlet.
H	high
HE	Heat engine
L	low
m	Mixed flow.
MC	mechanical compression

n	Nozzle.
o	Ambient.
p	Primary flow.
p1	Primary at section 1
py	primary at section y-y
s	Secondary or entrained flow.
sy	secondary at section y-y
t	Nozzle throat.
TVC	thermal vapour compression

**Super-scripts:**

1st	first law
Exergy	Exergy